



Research article

Effect of repeated freeze-thaw cycles on mechanical properties of clay

Haiqiang Jiang^{a,b,1}, Hongwei Han^{a,b,1}, Xingchao Liu^{a,b}, Enliang Wang^{a,b},
Qiang Fu^{a,b,*}, Jing Luo^{c,*}

^a School of Water Conservancy and Civil Engineering, Northeast Agricultural University, Harbin, 150030, China

^b Heilongjiang Provincial Key Laboratory of Water Resources and Water Conservancy Engineering in Cold Region, Northeast Agricultural University, Harbin, 150030, China

^c State Key Laboratory of Frozen Soil Engineering, Northwest Institute of Eco-Environment and Resources, Chinese Academy of Sciences, Lanzhou, 730000, China

ARTICLE INFO

Keywords:

Freeze-thaw cycles
Clay
Cohesion
Internal friction angle
Elastic modulus

ABSTRACT

To investigate the variation in the mechanical properties of clay under freeze-thaw cycles (FTCs), a series of experiments were conducted in the laboratory. Samples with different water contents and dry densities were subjected to FTCs ranging from 0 to 11 times. Then, cohesion, shear strength, internal friction angle and elastic modulus were obtained using triaxial test. The results show that with the increase in the number of FTCs, the shear strength, cohesion and elastic modulus decreased, while the internal friction angle increased slightly. However, the variation in the internal friction angle is not obvious, and the maximum increment is within 4°. The cohesion exhibited the most decrease after the first freeze-thaw action. Besides, under a same number of FTCs, four mechanical properties are significantly affected by water content and dry density. The shear strength, cohesion, elastic modulus and internal friction angle decrease with water content while increasing with dry density. Additionally, the elastic modulus is associated with confining pressure, which increases with confining pressure. This study provides evidence for the variation in mechanical properties of the soils subjected to FTCs and guides the design and construction of the cold regional engineering.

1. Introduction

Freeze-thaw cycles (FTCs) as a commonly weathering action that can occur more than 100 times within a year for the geological body in cold regions [1], which can change the properties of the soils and cause the engineering problems. Such as frost heave deformation [2,3] and thaw slumping [4–6], frost heave cracking of lining [7–9] and thermokarst [10,11]. Besides, the FTCs also can trigger many disasters including landslides and debris flow [12–14]. Unfortunately, the cold regions is widely distributed in the world, particularly it accounts for 43% of total land areas in China [15]. Therefore, the studies related to FTCs has drawn much attention by

* Corresponding author. State Key Laboratory of Frozen Soil Engineering, Northwest Institute of Eco-Environment and Resources, Chinese Academy of Sciences, Lanzhou, 730000 China.

** Corresponding author. School of Water Conservancy and Civil Engineering, Northeast Agricultural University, Harbin, 150030, China.

E-mail addresses: fuqiang0629@126.com (Q. Fu), luojing@lzb.ac.cn (J. Luo).

¹ Haiqiang Jiang and Hongwei Han contributed equally in this work.

<https://doi.org/10.1016/j.heliyon.2024.e27261>

Received 18 October 2023; Received in revised form 26 February 2024; Accepted 27 February 2024

Available online 28 February 2024

2405-8440/© 2024 The Authors. Published by Elsevier Ltd. This is an open access article under the CC BY-NC license (<http://creativecommons.org/licenses/by-nc/4.0/>).

the scientists and engineers to minimize its unfavorable impacts. As the mechanical properties of the soils is closely associated with the service ability of engineering and formation of disasters, most studies are conducted on the evolution of soils in mechanical and physical properties under repeated FTCs via laboratory experiment.

Shear strength and elastic modulus are two key mechanical factors, both of them are used to estimate the stability and guide the foundation design of the engineering. The cohesion and internal friction angle are necessary indexes for determining the shear strength, which are always obtained by triaxial test. Until now, many scholars have studied the mechanical properties of soils under FTCs in the lab about the above-mentioned factors. In terms of cohesion and internal friction angle, Liu et al. showed that the cohesion decreased after early FTCs and then kept stable after 9 FTCs. Meanwhile, the internal friction angle decreased at first and then increased during the FTCs, which reaches the minimum value after 7 FTCs [16]. However, some studies have drawn the different conclusions. Guo et al. considered that the variation in cohesion and internal friction angle of the soils subjected to FTCs always fluctuates [17]. Han et al. considered that the cohesion gradually decreases while the internal friction angle increases first then decreases with the increase in number of FTCs [18]. Kong et al. assumed that the variation stages of cohesion can be divided into two stages during the FTCs, including deteriorated stage when the number of FTCs ranged from 0 to 10 times and the stable stage when the number of FTCs ranged from 10 to 15 times [19]. Yao et al. analyzed the cohesion and internal friction angle of the soils after FTCs, and found that the variation of cohesion depended on the dry density. However, the variation of internal friction angle increased with the number of FTCs regardless of the dry density [20]. The similar researches about the cohesion and internal friction angle of the soils under FTCs also can be found in previously literatures [16,21–24]. In terms of the elastic modulus, Luo et al. conducted a series of tests and found that the elastic modulus decreases with the number of FTCs regardless the temperature [25]. Roman found that the properties of the morianic clayey loam were not changed significantly after 6 FTCs [26]. Yan et al. established a relationship between elastic modulus and number of FTCs of rocks by theoretical analysis, then analyzed the influence of frost heave and permeability coefficient on the elastic modulus [27]. Qu et al. investigated the elastic modulus of the soils with various water contents and dry densities after FTCs, and found that the elastic modulus are decreases with the number of FTCs regardless of the water content and dry density [28]. Clearly, in addition to the cohesion, the research conclusion about the variation of internal friction angle and elastic modulus of the soils under FTCs is contradict. As the amounts of water migration is driven by temperature gradient, different temperature controlling mode maybe a main reason for this difference. Until now, most experiments always set a constant positive temperature and a negative temperature in the FTCs process to simulate the air temperature variation [29–32]. Although there are many instruments can control temperature variation by linearly, the experiments are time consuming and the process is complex. Actually, the air temperature gradually varied instead of maintaining at a fixed value. Controlling the temperature as linearly varied can improve the similarity of the soils during the FTCs process between laboratory and in-situ, which can improve the accuracy of test results and provide credible scientific evidence for engineering practice.

Therefore, this study carried out a series of tests on the soil samples under FTCs. Particularly, the air temperature variation is controlled by linearity during the FTCs. After the samples were subjected to scheduled FTCs, the cohesion, internal friction angle as well as elastic modulus were measured and analyzed. The aims of this study are to: 1) analyze the effect of water content and dry density on shear strength, cohesion and internal friction angle as well as elastic modulus of the soils; 2) quantify the relationship between cohesion, internal friction angle, modulus and number of FTCs; and 3) reveal the effect of confining pressure on the elastic

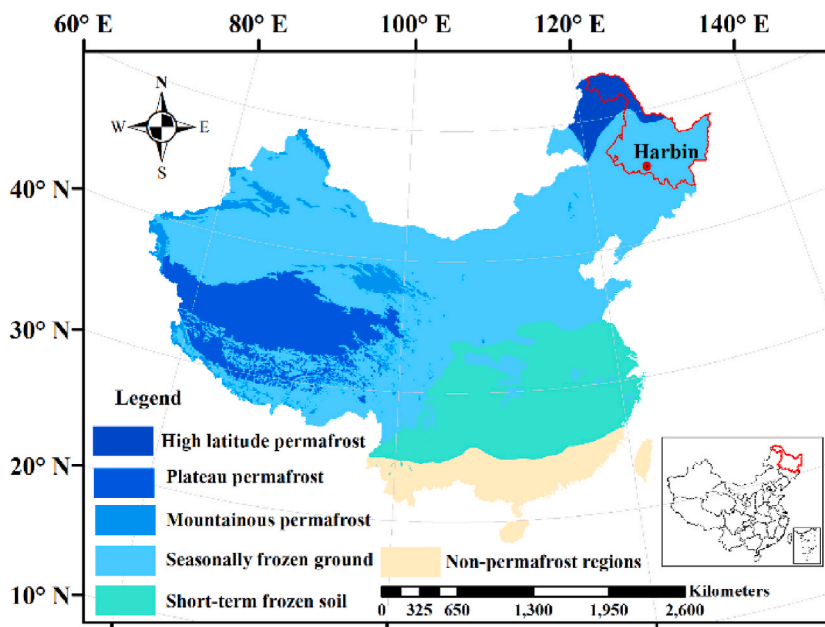


Fig. 1. Geographic information at study site [34].

modulus of the soils.

2. Laboratory experiments

2.1. Properties of soils

The soils were excavated in Harbin, which is governed by Heilongjiang Province and located on seasonally frozen ground, as shown in Fig. 1. The maximum frozen depth can reach 1.8 m. The mean air temperature is approximately 4 °C. The depth of the excavation ranges from 1.5 to 2 m. Based on the Standard for soils test method of China (GB/T 50123-2019) [33], the maximum dry density and optimal water content is 1.69 g/cm³ and 18.1%, respectively. The physical properties of the soil were measured and it can be classified as clay. The detailed properties can be found in Table 1 and in Fig. 2, respectively.

2.2. Test instruments and procedures

The FTCs were conducted in the low-temperature environment simulation laboratory with a dimension of 5 m × 4 m × 5 m (length × width × height). The key component of the laboratory consists of heating system, refrigeration system, water level control system and data record system. The designed temperature ranges from −40 °C to 50 °C. The surrounding structure is composed by insulation materials with the thickness of 25 cm and stainless steel with the thickness of 1 cm. The laboratory can carry out unidirectional freezing and bidirectional thawing processes to simulate the actual freeze-thaw process of the soil [35]. The soil samples with a dimension of 10 cm × 20 cm (diameter × height). In the freezing process, two compressors and condensing fins at the ceiling of the laboratory provide cold energy to freeze the samples. During in the thawing process, the electric heating rod and circulating oil at the bottom of the laboratory provide a thermal source to thaw the soil samples. The triaxial shear test was conducted by low-temperature frozen soil shear apparatus.

As the maximum dry density is 1.69 g/cm³, the dry density of the soil foundation in the construction should be around 1.60 g/cm³ based on the technical specifications [36]. On this basis, the dry density of the samples was 1.55 g/cm³, 1.60 g/cm³ and 1.65 g/cm³, respectively. In terms of the water content levels, as the optimal water content and saturated water content were approximately 18% and 27%, respectively. Therefore, the water content should also fall within this range, which was set as 18%, 20% and 22%, respectively. Firstly, the soils were crushed and passed through the sieve with an aperture of 2 mm. Then the initial water content was measured. Every sample was compacted into five layers. The interface between two adjacent layers was roughened to increase the integrity of the samples. After the sample was prepared, it was covered with an iron sheet with a thickness of 1 mm to prevent lateral deformation in the freezing process. Subsequently, the samples were putted into insulation holes with a diameter of 10 cm. Most studies indicated that the mechanical properties of the soils are stable when the number of FTCs ranging from 8 to 10 times [16,29,37]. Therefore, the number of FTCs was set as 0, 1, 3, 5, 7, 9 and 11 time(s), respectively in this study. After the samples were subjected to the scheduled FTCs, they were taken out and the unconsolidated and undrained triaxial shear tests were conducted. The shear rate is 1.5 mm/min and the confining pressures are 50 kPa, 100 kPa and 200 kPa, respectively. When the axial stress reaches the peak value or the axial strain reaches 15%–20%, the shearing process can be stopped. The experimental flowchart and some of prepared samples can be found in Fig. 3 and Fig. 4, respectively.

2.3. Temperature control mode

The air temperature variation process is divided into four stages based on the monitored data, including a continuous cooling stage (I), a constant negative temperature stage(II), a continuous warming stage(III) and a constant positive temperature(IV), as shown in Fig. 5. As the frozen depth is 1.8 m and the sample height is 0.2 m, the geometric scale is 1:9. Based on the similarity theory [38], the time scale is 1:81. The time consuming and temperature range in every stage during the FTCs are listed in Table 2.

It need to be emphasized that the samples were placed at 23.3 °C for 12 h before stage I to ensure a uniform temperature inside the samples.

3. Results and analysis

3.1. Shear strength

The stress-strain curves of the soil samples with a water content of 18% and a dry density of 1.65 g/cm³ were taken as examples to discuss the influence of FTCs on the shear strength. As seen in Fig. 6(a–g), the compression process consists of linear elastic stage,

Table 1
Basic parameters of the soils.

| Particle size analysis (μm) | | | | | Specific gravity | Liquid limit (%) | Plastic limit (%) | Plastic index (%) |
|-----------------------------|----------|------------|-------------|--------|------------------|------------------|-------------------|-------------------|
| sand | | | silt | | 2.69 | 44.9 | 23.0 | 21.9 |
| 2–0.5 | 0.5–0.25 | 0.25–0.075 | clay | | | | | |
| 0 | 0 | 0.7 | 0.075–0.005 | <0.005 | | | | |
| | | | 66.7 | 32.6 | | | | |

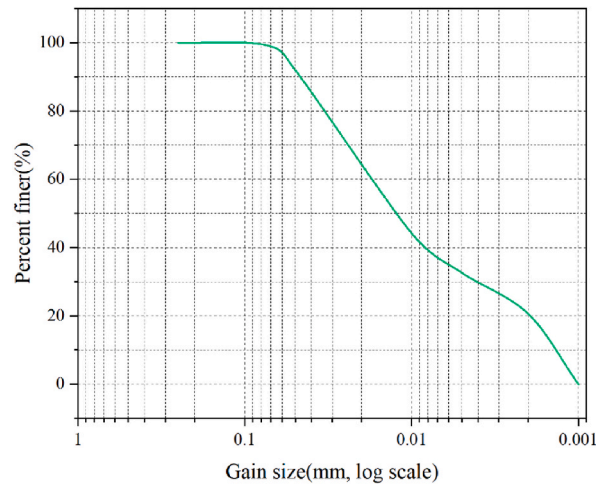


Fig. 2. Grain size distribution of clay.

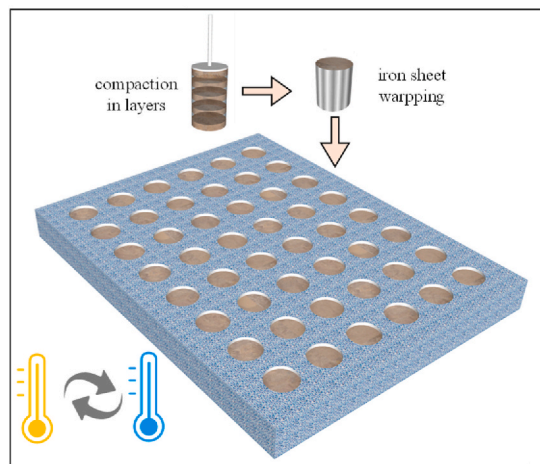


Fig. 3. Schematic diagram of experimental process.



Fig. 4. Prepared samples.

nonlinear stage and failure stage for every sample. The partially compressed samples can be found in Fig. 6(h–i). The number of FTCs and the confining pressure(p) significantly influence on shear strength. With an increase in number of FTCs, the shear strength gradually decreases under the same level of confining pressure due to the weakening of soil brittleness [39]. Additionally, as the confining pressure can increase the effective stress of the samples, the shear strength increases with confining pressure under a same number of FTCs. For example, the shear strength is 223 kPa ($p = 50$ kPa), 287 kPa ($p = 100$ kPa) and 344 kPa ($p = 200$ kPa), respectively when the samples FTCs is 0 (Fig. 6 (a)). However, these values are 205 kPa ($p = 50$ kPa), 252 kPa ($p = 100$ kPa) and 321

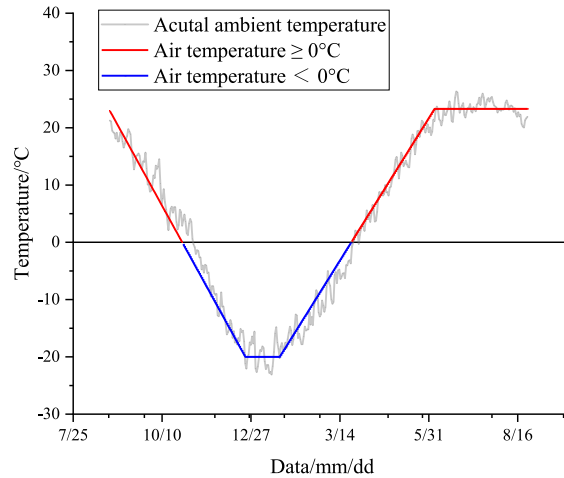


Fig. 5. The average air temperature variation from 2010 to 2012.

Table 2
Temperature controlling process during the experiments.

| Freeze-thaw stage | Date range (month/day) | Days | Time consumption after simplification (h) | Temperature range (°C) |
|-------------------|------------------------|------|---|------------------------|
| I | 8.26-12.22 | 119 | 27.58 | 23.3 ~ -20 |
| II | 12.23-1.22 | 30 | 6.95 | -20 ~ -20 |
| III | 1.23-6.5 | 135 | 31.25 | -20-23.3 |
| VI | 6.6-8.25 | 81 | 18.75 | 23.3-23.3 |

kPa ($p = 200$ kPa), respectively after 1 FTC (Fig. 6 (b)). Unit the FTCs reach 11 times, the shear strength are 130 kPa ($p = 50$ kPa), 150 kPa ($p = 100$ kPa) and 218 kPa ($p = 200$ kPa), respectively (Fig. 6 (g)). It suggests that the shear strength is affected not only by the confining pressure, but also by the number of FTCs. The greater the confining pressure, the higher the connectivity between soil grains, resulting in increased shear strength. However, the formation of ice crystals during the freezing process disrupts the connectivity between soil grains, leading to structural damage.

Furthermore, the shear strength of the samples under the confining pressure of 200 kPa after 11 FTCs is listed in Table 3 to illustrate the influences of dry density and water content. It is evident that the shear strength increases with the dry density while decreasing with water content. An increase in dry density increases the contact area between soil grains, thereby improving the shear strength. Meanwhile, higher moisture content results in a thicker water film around the grains, which decreases the ability of grains to resist shear force. This highlights the importance of water content and dry density as critical parameters in engineering construction, particularly for backfill soils. Controlling them within a specified range can improve the shear strength of the foundation.

3.2. Cohesion

Fig. 7(a-i) shows the cohesion of samples subjected to different numbers of FTCs. The cohesion of soils is affected by density, water content as well as number of FTCs. For example, when the soil samples with the water content of 18% and subjected to 1 FTC, the cohesion is 63.10 kPa (1.55 g/cm^3), 63.10 kPa (1.60 g/cm^3) and 92.67 kPa (1.65 g/cm^3), respectively (Fig. 7(a-c)). When the soil samples with the density of 1.60 g/cm^3 and the FTCs is 1 time, the cohesion is 71.56 kPa (18%), 50.39 kPa (20%), 38.28 kPa (22%), respectively (Fig. 7(d-f)). Similarly, when the soil samples with the density of 1.65 g/cm^3 and with the water content of 18%, the cohesion is 92.67 kPa(0 FTCs), 91.53 kPa(1 FTCs), 69.77 kPa(3 FTCs), 5.80 kPa(5 FTCs), 50.99 kPa(7 FTCs), 42.10 kPa(9 FTCs) and 41.90 kPa(11 FTCs), respectively (Fig. 7(g-i)). It can be found that the cohesion decreases with the increases in the number of FTCs for all samples. The cohesion mainly consists of Van der Waals forces, Coulomb forces and cementing forces. The strength of the contact surface between soil grains increases with increasing density. However, the water acts as a lubricant during the shear process, so the cohesion decreases with the increase in water content. Finally, the FTCs, as a weathering process, can degrade the soil's strength. In the freezing stage, the water phases into ice accompanied by an increase in volume. Meanwhile, the contact area between soil grains decreases and the distance between soil grains increase, resulting in decreases in Coulomb forces. Besides, some grains even break. It is worth mentioning that some of these changes cannot be restored during the thawing stage. Furthermore, as the number of FTCs increases, the pore area ratio also rises, causing the soil structure to become looser. This ultimately leads to degradation in cohesion [40]. Therefore, the water content, dry density and number of FTCs coupled determine the cohesion of soils. The relationship between the three factors is established, as shown in Eq. (1).

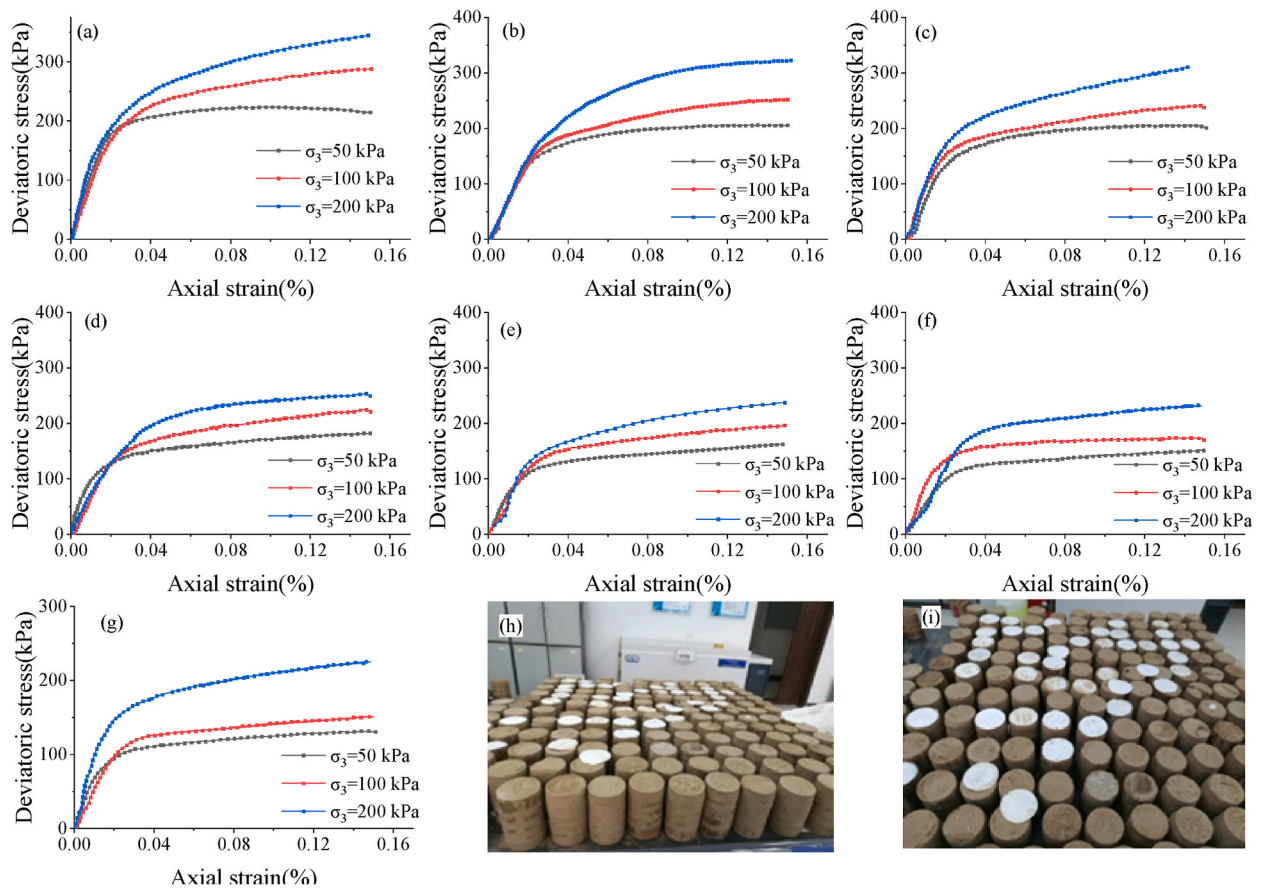


Fig. 6. The relationship between the deviatoric stress and axial strain of the samples (a)–(g): The FTCs is 0,1,3,5,7,9,11, respectively; (h) and (i) is partially compressed samples.

Table 3

The shear strength of the samples with the confining pressure of 200 kPa after 11 FTCs.

| Water content (%) | Dry density(g/cm ³) | Shear strength (kPa) |
|-------------------|---------------------------------|----------------------|
| 18 | 1.55 | 180 |
| 18 | 1.60 | 192 |
| 18 | 1.65 | 218 |
| 20 | 1.65 | 181 |
| 22 | 1.65 | 118 |

$$y_c = e^{(-8.65x_1 + 4.79x_2 - 17.27x_3 - 0.21)} \quad R^2 = 0.94 \tag{1}$$

where y_c is the cohesion; x_1 , x_2 and x_3 represents the number of FTCs, dry density and water content, respectively. In this study, the values of x_1 , x_2 and x_3 equals to -8.65 , 4.79 and -17.27 , respectively.

3.3. Internal friction angle

The variation in internal friction angle of the samples is shown in Fig. 8(a–i). The internal friction angle is related to water content and dry density as well as the number of FTCs. The internal friction angle reflects the surface friction force of soil grains and the connection strength between soil grains. Clearly, the internal friction angle increases with dry density and number of FTCs while it decreases with water content. For the samples with the water content of 18% and subjected to 3 FTCs, the internal friction angles are 14.78° (1.55 g/cm³), 17.26° (1.60 g/cm³), 18.12° (1.65 g/cm³), respectively (Fig. 8(a–c)). For the samples with a fixed dry density and number of FTCs, the internal friction angle decreases with increasing water content. When the dry density is 1.60 g/cm³ and the number of FTCs is 5 times, the internal friction angles are 17.20° (18%), 14.58° (20%), 12.21° (22%), respectively (Fig. 8 (b), (e) and (h)). This is because the thicker water film can reduce the friction force between soil grains, so that the grains are easier to be moved

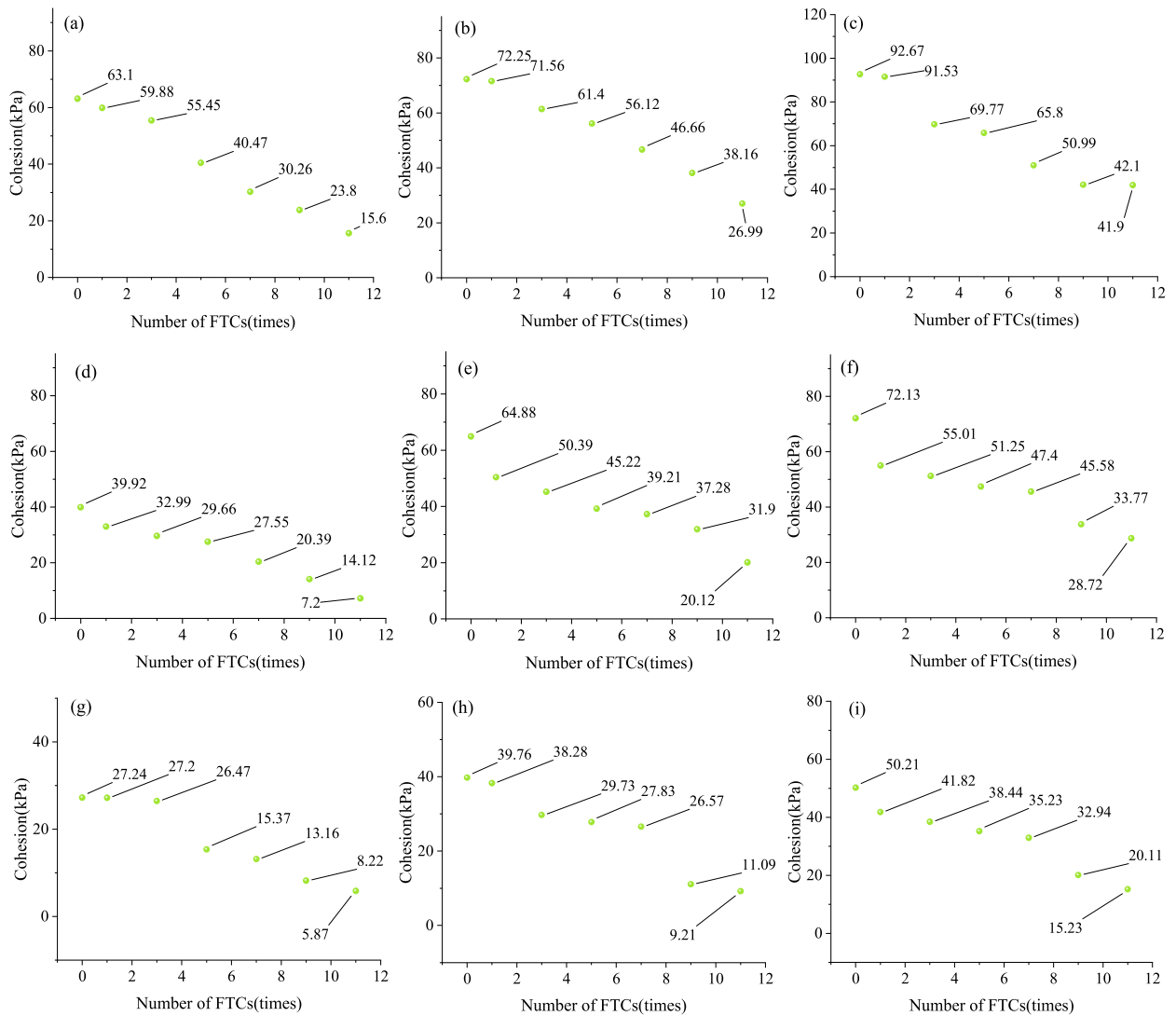


Fig. 7. Cohesion of the samples after different FTCs (a): $w = 18\%$, $\rho = 1.55 \text{ g/cm}^3$; (b): $w = 18\%$, $\rho = 1.60 \text{ g/cm}^3$; (c): $w = 18\%$, $\rho = 1.65 \text{ g/cm}^3$; (d): $w = 20\%$, $\rho = 1.55 \text{ g/cm}^3$; (e): $w = 20\%$, $\rho = 1.60 \text{ g/cm}^3$; (f): $w = 20\%$, $\rho = 1.65 \text{ g/cm}^3$; (g): $w = 22\%$, $\rho = 1.55 \text{ g/cm}^3$; (h): $w = 22\%$, $\rho = 1.60 \text{ g/cm}^3$; (i): $w = 22\%$, $\rho = 1.65 \text{ g/cm}^3$.

under the loading. In essence, the sliding friction force and occlusal friction force between soil grains are reduced under high water content. However, the internal friction angle increases with the increase in dry density for the samples with a fixed water content and number of FTCs. When the water content is 22% and the number of FTCs is 7 times, the internal friction angle is 11.33° (1.55 g/cm^3), 12.82° (1.60 g/cm^3), 13.05° (1.65 g/cm^3), respectively (Fig. 8(g–i)). As the dry density increased, the contact area between the grains increased, which enhanced the strength of the soil skeleton. Then the ability of the soil grains to resist relative sliding is also improved under the loading, thus the internal friction angle is increased. Additionally, the internal friction angle of all samples increases with the number of FTCs. For the samples with a water content of 18%, the increment of internal friction angle after it was subjected to 11 FTCs is 2.10° (1.55 g/cm^3), 3.26° (1.60 g/cm^3), 2.58° (1.65 g/cm^3), respectively (Fig. 8(a–c)). While for the samples with water content of 20% and 22%, the increment of internal friction angle after it was subjected to 11 times of FTCs are 3.00° (1.55 g/cm^3), 1.64° (1.60 g/cm^3), 1.58° (1.65 g/cm^3), 2.43° (1.55 g/cm^3), 2.43° (1.60 g/cm^3), 2.59° (1.65 g/cm^3), respectively (Fig. 8(d–i)). The reason for the increment in the internal friction angle may be associated with the degree of circularity of the soil grains [40]. With the increase in the number of FTCs, the degree of circularity of the soil grains decreases, and the soil grains tend to become uneven. This results in a stronger friction force. Therefore, the internal friction angle shows an increasing trend with the increase in FTCs. As the internal friction angle is affected by water content, dry density and number of FTCs, the quantitative relationship between them is established, as shown in Eq. (2).

$$y_f = e^{(1.47x_1 + 1.52x_2 - 8.60x_3 + 1.85)} \quad R^2 = 0.95 \quad (2)$$

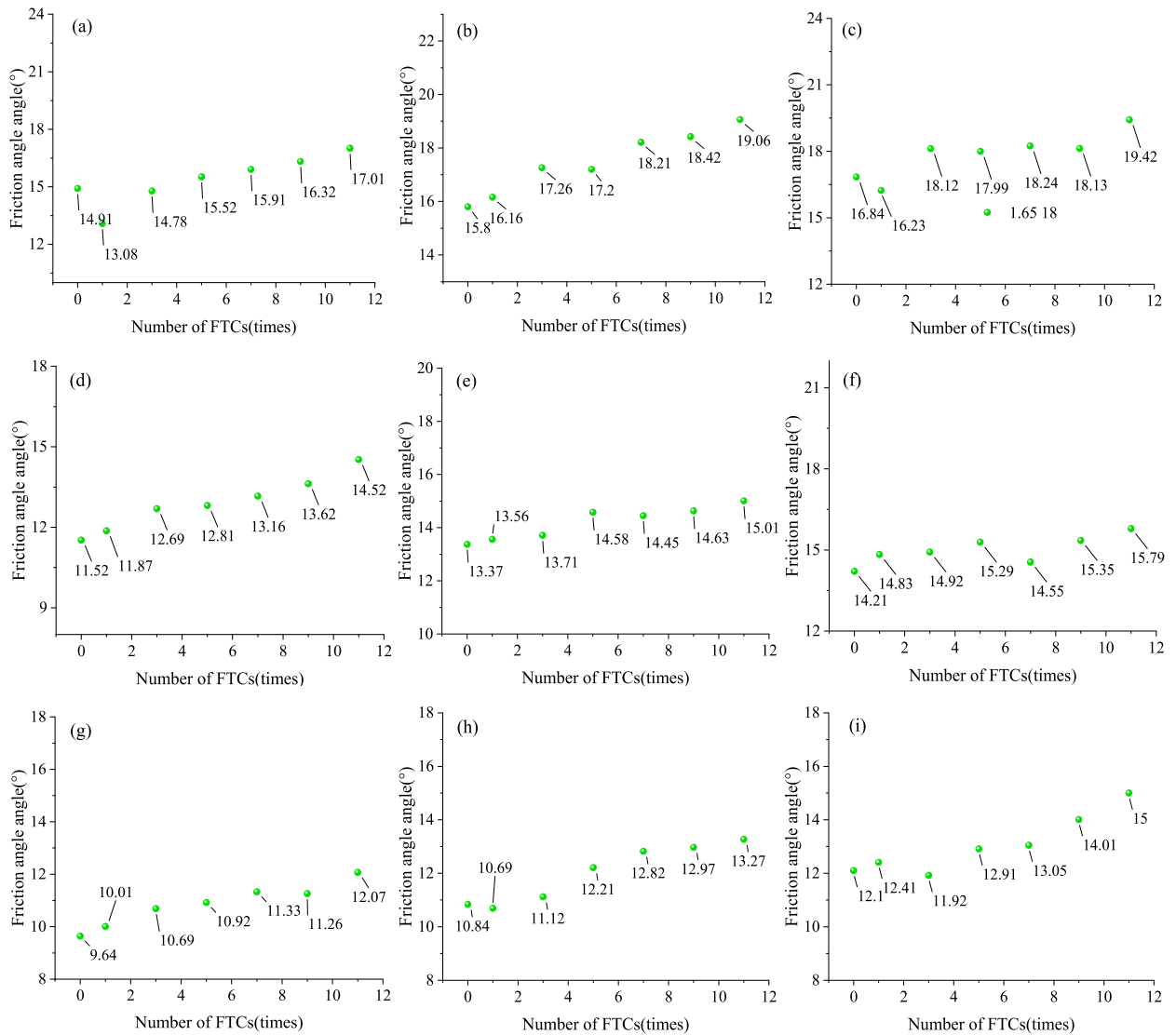


Fig. 8. Internal friction angle of the samples after different FTCs. (a): $w = 18\%$, $\rho = 1.55 \text{ g/cm}^3$; (b): $w = 18\%$, $\rho = 1.60 \text{ g/cm}^3$; (c): $w = 18\%$, $\rho = 1.65 \text{ g/cm}^3$; (d): $w = 20\%$, $\rho = 1.55 \text{ g/cm}^3$; (e): $w = 20\%$, $\rho = 1.60 \text{ g/cm}^3$; (f): $w = 20\%$, $\rho = 1.65 \text{ g/cm}^3$; (g): $w = 22\%$, $\rho = 1.55 \text{ g/cm}^3$; (h): $w = 22\%$, $\rho = 1.60 \text{ g/cm}^3$; (i): $w = 22\%$, $\rho = 1.65 \text{ g/cm}^3$.

where y_f is the internal friction angle; x_1 , x_2 and x_3 represents the number of FTCs, dry density and water content, respectively. In this study, the values of x_1 , x_2 and x_3 equals to 1.47, -8.60 and 1.85, respectively.

3.4. Elastic modulus

The elastic modulus represents the ability of soil to resist elastic deformation. The determination of the elastic modulus is based on the relationship between deviatoric stress and axial strain. By fitting linear segments in the curves between deviatoric stress and axial strain, the slope is determined as elastic modulus [41]. To accurately quantify the variation of elastic modulus, a dimensionless D_{Ei} is defined to describe its deterioration.

$$D_{Ei} = \frac{D_0 - D_i}{D_0} \times 100\% \tag{3}$$

where D_{Ei} is the elastic modulus deterioration ratio and i is the number of FTCs.

The elastic modulus of the samples under different confining pressures is shown in Fig. 9(a–c). It is obvious that the water content and dry density as well as number of FTCs affect the elastic modulus. The elastic modulus increases with the dry density and decreases

with the water content. After 1 FTC, the elastic modulus is 6.69 MPa (1.55 g/cm³), 11.49 MPa (1.60 g/cm³), 14.81 MPa (1.65 g/cm³) for the samples with the water content of 18%, respectively (Fig. 9 (a)). While it is 5.91 MPa (1.55 g/cm³), 8.90 MPa (1.60 g/cm³), 10.02 MPa (1.65 g/cm³) for the samples with a water content of 20%, respectively (Fig. 9 (b)). Similarly, it is 4.16 MPa (1.55 g/cm³), 5.35 MPa (1.60 g/cm³), 5.96 MPa (1.65 g/cm³) for the samples with a water content of 22%, respectively (Fig. 9 (c)). The reason for this is that the soil grains inside the samples with a high dry density are much denser than those with a low dry density, which results in the samples possessing a good ability to resist elastic deformation. However, when the samples with the dry density of 1.55 g/cm³ while the FTCs is 3 times, the elastic modulus is 6.48 MPa (18%), 5.67 MPa (20%) and 4.07 MPa (22%), respectively. The increase in water content causes the bound water film to be thicker while decreasing the Van der Waals force. At this situation, the energy required to fracture is smaller than the chemical bonding force between the soil skeleton at low water content. Therefore, water content essentially reduces the elastic modulus by impairing the bonding strength between soil grains.

The elastic modulus significantly decreases after 1 FTC, then slightly increases and finally decreases again. The modulus increased when the number of FTCs ranged from 3 to 5 times. The reason for this is that the elastic modulus is associated with the size of soil grains [42]. The original soil grains break into finer grains after 1 FTC, which leads to an increase in porosity and makes the soil more prone to deformation. This is evidenced at a macroscopic level by a decrease in elastic modulus. Subsequently, the finer grains gradually agglomerate into larger grains when FTCs range from 3 to 5 times. At the same time, a reduction in porosity contributes to an increase in the elastic modulus of the soil sample. Then, the larger grains break again with the increases of FTCs, which resulting in a reduction in elastic modulus. After the samples were subjected to 1 FTC, the modulus significantly decreased regardless of the water content and dry density. For example, when the samples with a dry density of 1.55 g/cm³ and a confining pressure of 50 kPa, the D_{E1} is 48% (18%), 37% (20%) and 38% (22%), respectively. When the samples with a water content of 18% and a confining pressure of 50 kPa, the D_{E1} is 23% (1.60 g/cm³) and 36% (1.65 g/cm³), respectively. After the samples were subjected to 11 FTCs, the D_{E11} under different confining pressures are listed in Table 4. The minimum D_{E11} is 47.9% (water content of 20% and dry density of 1.60 g/cm³), 51.3% (water content of 20% and dry density of 1.60 g/cm³) and 57% (water content of 20% and dry density of 1.65 g/cm³) when the confining pressure of 50 kPa, 100 kPa and 200 kPa, respectively. It can be seen that the FTCs can cause the elastic modulus to decrease when compared with the samples that have not been subjected to FTCs. As the elastic modulus determines the deformation of engineering, the deformation should be strictly noticed within 1 year after it has been constructed.

Besides, the confining pressure is also a key factor in determining the elastic modulus. The elastic modulus of samples under confining pressures of 100 kPa and 200 kPa are shown in Fig. 10(a–f). Clearly, the elastic modulus increases with the increase in confining pressure. The confining pressure can effectively restrict the lateral deformation of the samples, so the modulus is improved accordingly.

4. Conclusions

This study conducted a temperature control mode based on similarity theory instead of traditional temperature control methods. Then, a series of FTCs were conducted on the soil samples with different initial conditions. The main mechanical properties including shear strength, cohesion and internal friction angle as well as elastic modulus were measured and analyzed. The main findings of this study are as follows:

- (1) The cohesion, shear strength, elastic modulus and internal friction angle are affected by FTCs. The cohesion and shear strength of the soils decrease and the internal friction angle increases after FTCs. However, the increment in internal friction angle is not obvious, which is always less than 4°. The degradation in cohesion and elastic modulus can reduce the stability of the engineering foundation in cold regions. Therefore, measures to mitigate the effects of FTCs should be taken into account in the engineering design process.
- (2) For the samples subjected to the same number of FTCs, the cohesion, internal friction angle and elastic modulus are affected by the water content and dry density. When the water content is constant, the cohesion and internal friction angle increase with the increase in dry density. When the dry density is constant, the cohesion and internal friction angle decrease with the increase in water content. Therefore, it is necessary to control the water content and dry density of the soils for engineering infrastructure in cold regions, such as reinforcing the foundation and strengthening the drainage.
- (3) The elastic modulus of the soils increases with the confining pressure. Besides, the elastic modulus significantly decreases after 1 FTC regardless of the water content and dry density, then slightly increases when the number of FTCs ranged from 3 to 5 times and finally decreases again. As the reduction in elastic modulus increases the risk of structure overturning and settlement in long-term service, the monitoring of the deformations should be implemented during the service life of the engineering in cold regions.

Data availability statement

Data will be made available on request.

CRediT authorship contribution statement

Haiqiang Jiang: Writing – review & editing, Writing – original draft, Methodology, Investigation, Funding acquisition, Formal analysis, Conceptualization. **Hongwei Han:** Writing – review & editing, Writing – original draft, Investigation, Formal analysis,

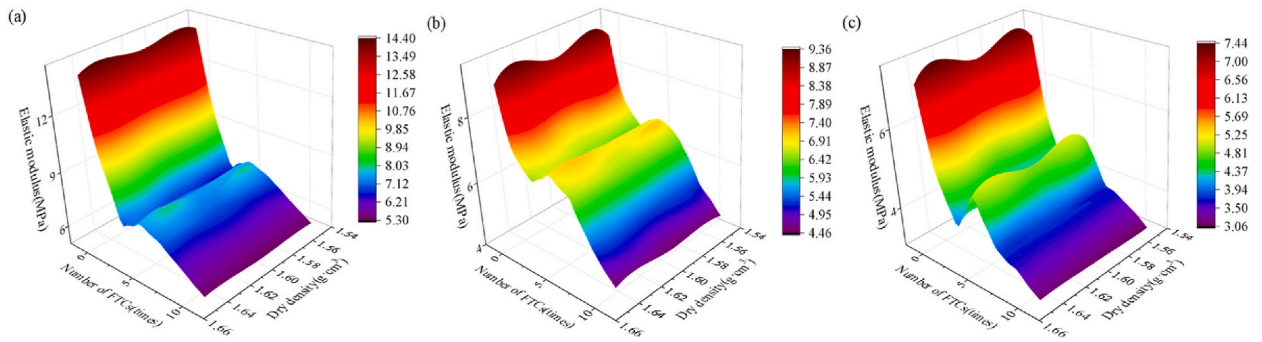


Fig. 9. Elastic modulus of the samples after different FTCs (I) (a): $w = 18\%$, $p = 50$ kPa; (b): $w = 20\%$, $p = 50$ kPa; (c): $w = 22\%$, $p = 50$ kPa.

Table 4

The values of D_{E11} under different confining pressures.

| Water content (%) | Dry density(g/cm ³) | D_{E11} (%) | | |
|-------------------|---------------------------------|---------------|------|------|
| | | 50 | 100 | 200 |
| 18 | 1.55 | 61.8 | 64.9 | 60.4 |
| 18 | 1.60 | 57.6 | 70.8 | 67.8 |
| 18 | 1.65 | 70.6 | 69.7 | 67.1 |
| 20 | 1.55 | 60.3 | 59.8 | 57.3 |
| 20 | 1.60 | 47.9 | 51.3 | 61.8 |
| 20 | 1.65 | 50.9 | 52.6 | 57.0 |
| 22 | 1.55 | 65.3 | 64.1 | 64.1 |
| 22 | 1.60 | 51.9 | 59.3 | 62.0 |
| 22 | 1.65 | 62.0 | 62.9 | 62.6 |

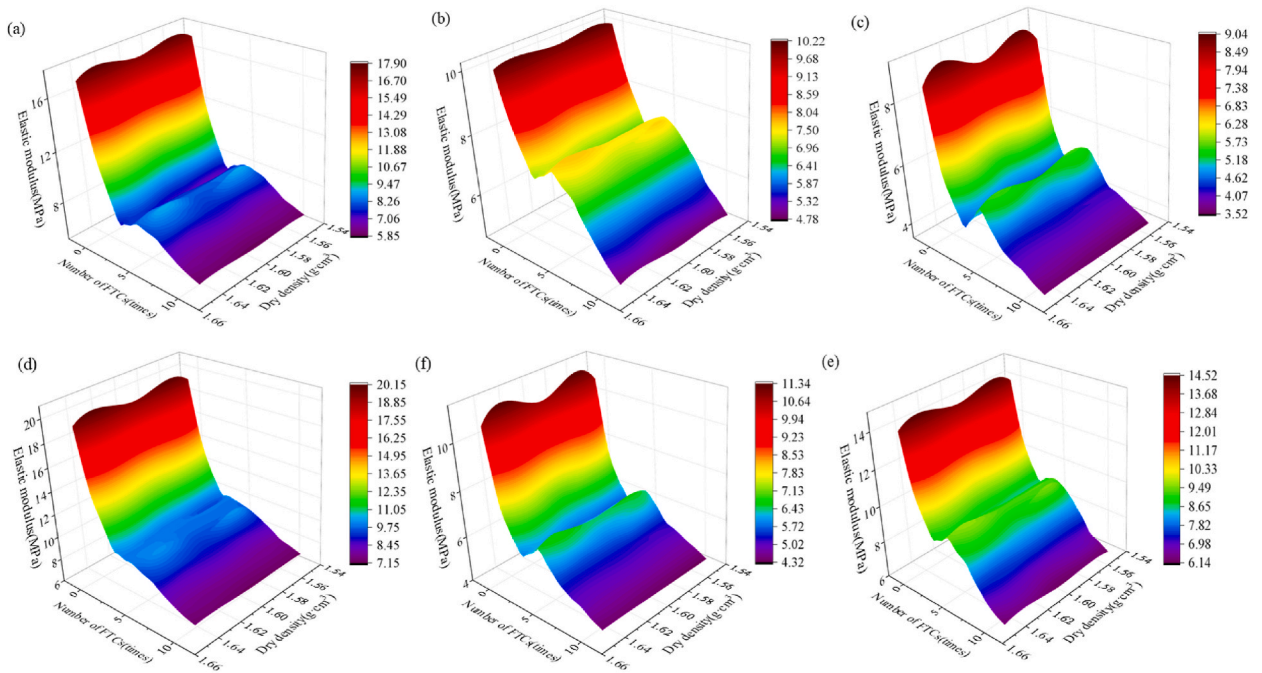


Fig. 10. Elastic modulus of the samples after different FTCs (II) (a): $w = 20\%$, $p = 100$ kPa; (b): $w = 20\%$, $p = 100$ kPa; (c): $w = 20\%$, $p = 100$ kPa; (d): $w = 22\%$, $p = 200$ kPa; (e): $w = 22\%$, $p = 200$ kPa; (f): $w = 22\%$, $p = 200$ kPa.

Conceptualization. **Xingchao Liu**: Writing – original draft, Formal analysis. **Enliang Wang**: Writing – original draft, Investigation, Funding acquisition, Formal analysis, Conceptualization. **Qiang Fu**: Supervision, Methodology, Investigation, Formal analysis. **Jing Luo**: Writing – original draft, Methodology, Investigation, Funding acquisition, Formal analysis.

Declaration of competing interest

The authors declare that they have no known competing financial interests or personal relationships that could have appeared to influence the work reported in this paper.

Acknowledgments

This work was supported by the National Science Foundation of China (Grant No. U2268216), Major Scientific and Technological Projects of the Ministry of Water Resources (Grant No. SKS-2022017) and Heilongjiang Provincial Post-doctoral Science Foundation (Grant No. LBH-Z22073). The authors would like to thank the editors and anonymous reviewers for their valuable comments and suggestions.

References

- [1] N. Hosokawa, K. Isobe, R. Urakawa, R. Tatenno, K. Fukuzawa, T. Watanabe, H. Shibata, Soil freeze–thaw with root litter alters N transformations during the dormant season in soils under two temperate forests in northern Japan, *Soil Biol. Biochem.* 114 (2017) 270–278.
- [2] H. Zheng, S. Kanie, F.J. Niu, A.Y. Li, Three-dimensional frost heave evaluation based on practical Takashi's equation, *Cold Reg. Sci. Technol.* 118 (2015) 30–37.
- [3] F.J. Niu, H. Zheng, A.Y. Li, The study of frost heave mechanism of high-speed railway foundation by field-monitored data and indoor verification experiment, *Acta. Geotech.* 15 (2020) 581–593.
- [4] A.J. Houben, T.D. French, S.V. Kokelj, X.W. Wang, J.P. Smol, J.M. Blais, The impacts of permafrost thaw slump events on limnological variables in upland tundra lakes, Mackenzie Delta region, *Fund. Appl. Limnol.* 189 (2016) 11–35.
- [5] J. Luo, F.J. Niu, Z.J. Lin, M.H. Liu, G.A. Yin, Recent acceleration of thaw slumping in permafrost terrain of Qinghai-Tibet Plateau: an example from the Beiluhe Region, *Geomorphology* 341 (2019) 79–85.
- [6] A.I. Kizyakov, S. Wetterich, F. Günther, T. Opel, L.L. Jongejans, J. Courtin, H. Meyer, A.G. Shepelev, I.I. Syromyatnikov, A.N. Fedorov, Landforms and degradation pattern of the Batagay thaw slump, Northeastern Siberia, *Geomorphology* 420 (2023) 108501, 2023.
- [7] H.Q. Jiang, F.J. Niu, Q.G. Ma, W.J. Su, E.L. Wang, J.L. He, Numerical analysis of heat transfer between air inside and outside the tunnel caused by piston action, *Int. J. Therm. Sci.* 170 (2021) 107164.
- [8] J.B. Zhu, D.D. Xu, B. Wang, C. Li, A study on the freeze–thaw damage and deterioration mechanism of slope rock mass based on model testing and numerical simulation, *Appl. Sci.* 12 (2022) 6545.
- [9] S. Huang, J. Wang, Y.Z. Liu, Q. Tian, C. Cai, Experimental investigation on crack coalescence and strength loss of rock-like materials containing two parallel water-filled flaws under freeze–thaw, *Theor. Appl. Fract. Mech.* 123 (2023) 103669.
- [10] Z.Y. Gao, F.J. Niu, Z.J. Lin, Effects of permafrost degradation on thermokarst lake hydrochemistry in the Qinghai-Tibet Plateau, China, *Hydrol. Process.* 34 (2020) 5659–5673.
- [11] Z.Y. Gao, F.J. Niu, Z.J. Lin, J. Luo, G.A. Yin, Y.B. Wang, Evaluation of thermokarst lake water balance in the Qinghai-Tibet Plateau via isotope tracers, *Sci. Total Environ.* 636 (2018) 1–11.
- [12] H. Nagai, K. Fujita, T. Nuimura, A. Sakai, Southwest-facing slopes control the formation of debris-covered glaciers in the Bhutan Himalaya, *Cryosphere* 7 (2013) 1303–1314.
- [13] G.A. Yin, J. Luo, F.J. Niu, Z.J. Lin, M.H. Liu, Machine learning-based thermokarst landslide susceptibility modeling across the permafrost region on the Qinghai-Tibet Plateau, *Landslides* 18 (2021) 2639–2649.
- [14] C. Ma, K.H. Hu, S. Liu, J.L. Wu, Recent two runoff-triggered debris flow events in Tibet Plateau, China, *Landslides* 19 (2022) 2409–2422.
- [15] Z.N. Yang, X.R. Liu, Q.Z. Zeng, *Hydrology in Cold Regions of China*, Science Press, 2000.
- [16] J.K. Liu, D. Chang, Q.M. Yu, Influence of freeze-thaw cycles on mechanical properties of a silty sand, *Eng. Geol.* 210 (2016) 23–32.
- [17] Z.K. Guo, Z.Z. Zhang, Y.X. Mu, T. Li, Y.Y. Zhang, G.M. Shi, Effect of freeze-thaw on mechanical properties of loess with different moisture content in Yili, Xinjiang, *Sustainability* 14 (2022) 11357.
- [18] Y. Han, Q. Wang, N. Wang, J.Q. Wang, X.D. Zhang, S.K. Cheng, Y.Y. Kong, Effect of freeze-thaw cycles on shear strength of saline soil, *Cold Reg. Sci. Technol.* 154 (2018) 42–53.
- [19] F.S. Kong, L. Nie, Y. Xu, X.J. Rui, Y.Y. He, T. Zhang, Y.Z. Wang, C. Du, C.H. Bao, Effects of freeze-thaw cycles on the erodibility and microstructure of soda-saline loessal soil in Northeastern China, *Catena* 209 (2022) 105812, 2022.
- [20] X.L. Yao, L.L. Fang, J.L. Qi, F. Yu, Study on mechanism of freeze-thaw cycles induced changes in soil strength using electrical resistivity and x-ray computed tomography, *J. Offshore Mech. Arct.* 139 (2017) 02150.
- [21] W.T. Chen, Y. Wang, M.N. Wang, S. Li, Y.S. Wang, Testing study on influence of freezing and thawing circulation on saline soil's cohesion, *Rock Soil Mech.* 28 (2007) 2343–2347.
- [22] Y.Q. Sun, S.J. Meng, M. Wang, H.L. Mu, X.C. Tang, Deterioration effect of freeze-thaw on mechanical properties of roadbed clay under unfavorable conditions, *Bull. Eng. Geol. Environ.* 80 (2021) 4773–4790.
- [23] M. Wang, S.J. Meng, Y.Q. Sun, H.Q. Fu, Shear strength of frozen clay under freezing-thawing cycles using triaxial tests, *Earthq. Eng. Eng. Vib.* 17 (2018) 761–769.
- [24] B. Wang, J.H. Gao, Y.Q. Wang, X.J. Quan, Y.W. Gong, S.W. Zhou, Experimental study on the effect of freezing and thawing on the shear strength of the frozen soil in Qinghai-Tibet railway embankment, *Adv. Civ. Eng.* (2022) 1–12.
- [25] X. Luo, S. Zhou, B. Huang, N. Jiang, M. Xiong, Effect of freeze–thaw temperature and number of cycles on the physical and mechanical properties of marble, *Geotech. Geol. Eng.* 39 (2021) 567–582.
- [26] L.T. Roman, Z. Zhang, Effect of freezing-thawing on the physico-mechanical properties of a Morianic clayey loam, *Soil Mech. Found. Eng.* 47 (2010) 96–101.
- [27] X.D. Yan, H.Y. Liu, C.F. Xing, C. Li, Variability of elastic modulus in rock under freezing-thawing cycles, *Rock Soil Mech.* 36 (2015) 2315–2322.
- [28] Y.L. Qu, W.K. Ni, F.J. Niu, Y.H. Mu, G.L. Chen, J. Luo, Mechanical and electrical properties of coarse-grained soil affected by cyclic freeze-thaw in high cold regions, *J. Cent. South Univ.* 27 (2020) 853–866.
- [29] D.Y. Wang, W. Ma, Y.H. Niu, X.X. Chang, Z. Wen, Effects of cyclic freezing and thawing on mechanical properties of Qinghai-Tibet clay, *Cold Reg. Sci. Technol.* 48 (2007) 34–43.
- [30] E. Kravchenko, J.K. Liu, A. Krainiukov, D. Chang, Dynamic behavior of clay modified with polypropylene fiber under freeze-thaw cycles, *Transp. Geotech.* 21 (2019) 100282.
- [31] M.E. Orakoglu, J.K. Liu, F.J. Niu, Dynamic behavior of fiber-reinforced soil under freeze-thaw cycles, *Soil Dynam. Earthq. Eng.* 101 (2017) 269–284.
- [32] X.Q. Liu, J.K. Liu, Y.H. Tian, Y.P. Shen, D. Chang, The mechanical properties of lean clay filler under freeze-thaw and thermostatic curing cycles in loess plateau, *KSCE J. Civ. Eng.* 27 (2023) 1470–1479.
- [33] GB/T 50123-2019, Standard for geotechnical testing method (2019).
- [34] Y.H. Ran, X. Li, G.D. Cheng, T.J. Zhang, Q.B. Wu, H.J. Jin, R. Jin, Distribution of permafrost in China: an overview of existing permafrost maps, *Permafrost Periglac.* 23 (2012) 322–333.

- [35] E.L. Wang, H.Q. Jiang, D.K. Li, X.C. Liu, C. Zhang, D. Zhang, Development and application of simulation chamber for freezing and thawing cycle, *Cryo. Supercond* 45 (2017) 86–91.
- [36] DB64T 811-2012, Technical specifications for irrigation channel lining engineering (2012).
- [37] M.E. Orakoglu, J. Liu, Effect of freeze-thaw cycles on triaxial strength properties of fiber-reinforced clayey soil, *KSCE J. Civ. Eng.* 21 (2017) 2128–2140.
- [38] D.Q. Li, Freeze-thaw Model Test and its Similarity Analysis (Phdthesis), Lanzhou Institute of Glaciology and Frozen Soil, Chinese Academy of Sciences, Lanzhou, 1993.
- [39] T.F. Hu, J.H. Fang, D. Chang, D.W. Liu, Experimental study on the effect of cyclic freezing-thawing on mechanical properties of silty clay with different degrees of compaction, *Chin. J. Rock Mech. Eng.* 36 (2017) 1495–1503.
- [40] Q. Wang, J. Qi, S. Wang, J. Xu, Y. Yang, Effect of freeze-thaw on freezing point of a saline loess, *Cold Reg. Sci. Technol.* 170 (2020) 102922.
- [41] J. Wang, H.B. Liu, C.L. Wu, Influence of freeze-thaw cycles on elastic modulus of subgrade soil with different plasticity indices, *Rock Soil Mech.* 33 (2012) 3665–3668.
- [42] D.Y. Wang, W. Ma, X.X. Chang, Z.Z. Sun, W.J. Feng, J.W. Zhang, Physico-mechanical properties changes of Qinghai-Tibet clay due to cyclic freezing and thawing, *Chin. J. Rock Mech. Eng.* 24 (2005) 4313–4319.